



Adaption of the  
MODIS aerosol  
retrieval algorithm

E. Jäkel et al.

This discussion paper is/has been under review for the journal Atmospheric Measurement Techniques (AMT). Please refer to the corresponding final paper in AMT if available.

# Adaption of the MODIS aerosol retrieval algorithm by airborne spectral surface reflectance measurements over urban areas: a case study

E. Jäkel<sup>1</sup>, B. Mey<sup>1,2</sup>, R. Levy<sup>3</sup>, X. Gu<sup>4</sup>, T. Yu<sup>4</sup>, Z. Li<sup>4</sup>, D. Althausen<sup>5</sup>, B. Heese<sup>5</sup>, and M. Wendisch<sup>1</sup>

<sup>1</sup>Institute for Meteorology, University of Leipzig, Stephanstr. 3, 04103 Leipzig, Germany

<sup>2</sup>Fraunhofer Institute for Wind Energy and Energy System Technology, Königstor 59, 34119 Kassel, Germany

<sup>3</sup>NASA/GSFC Code 613, Greenbelt, MD 20771, USA

<sup>4</sup>Institute of Remote Sensing and Digital Earth, Chinese Academy of Sciences, No. 20 Datun Road, Chaoyang District, Beijing 100101, China

<sup>5</sup>Leibniz Institute for Tropospheric Research, Permoserstr. 15, 04318 Leipzig, Germany

Received: 11 May 2015 – Accepted: 30 June 2015 – Published: 16 July 2015

Correspondence to: E. Jäkel (e.jaekel@uni-leipzig.de)

Published by Copernicus Publications on behalf of the European Geosciences Union.

|                          |              |
|--------------------------|--------------|
| Title Page               |              |
| Abstract                 | Introduction |
| Conclusions              | References   |
| Tables                   | Figures      |
| ◀                        | ▶            |
| ◀                        | ▶            |
| Back                     | Close        |
| Full Screen / Esc        |              |
| Printer-friendly Version |              |
| Interactive Discussion   |              |



## Abstract

MODIS retrievals of the aerosol optical depth (AOD) are biased over urban areas, where surface reflectance is not well characterized. Since the operational MODIS aerosol retrieval for dark targets assumes fixed spectral slopes to calculate the surface reflectance at  $0.47\ \mu\text{m}$ , the algorithm may fail in urban areas with different spectral characteristics of the surface reflectance. To investigate this bias we have implemented variable spectral slopes into the operational MODIS aerosol algorithms of Collection 5 (C5) and C6. The variation of slopes is based on airborne measurements of surface reflectances over the city of Zhongshan, China. AOD retrieval results of the operational and the modified algorithms were compared for a MODIS measurement over Zhongshan. For this case slightly lower AOD values were derived using the modified algorithm. The retrieval methods were additionally applied to MODIS data of the Beijing area for a period between 2010–2014 when also AERONET data were available. A reduction of the differences between the AOD retrieved using the modified C5 algorithm and AERONET was found, whereby the mean difference from  $0.31 \pm 0.11$  for the operational C5 and  $0.18 \pm 0.12$  for the operational C6 were reduced to a mean difference of  $0.09 \pm 0.18$  by using the modified C5 retrieval. Furthermore, the sensitivity of the MODIS AOD retrieval for several surface types was investigated. Radiative transfer simulations were performed to model reflectances at top of atmosphere for predefined aerosol properties. The reflectances were used as input for the retrieval methods. It is shown that the operational MODIS AOD retrieval over land reproduces the AOD reference input of 0.85 for dark surface types [retrieved AOD = 0.87 (C5)]. An overestimation of AOD = 0.99 is found for urban surfaces, whereby the modified C5 algorithm shows a good performance with a retrieved value of AOD = 0.86.

## Adaption of the MODIS aerosol retrieval algorithm

E. Jäkel et al.

Title Page

Abstract

Introduction

Conclusions

References

Tables

Figures



Back

Close

Full Screen / Esc

Printer-friendly Version

Interactive Discussion



## 1 Introduction

Aerosol particles influence various branches of the Earth's ecosystem. By scattering (Charlson et al., 1987, 1992; Tegen et al., 2000) or absorbing (Jacobson, 2001; Ramanathan et al., 2001) of solar radiation aerosol particles influence the Earth's radiation budget and the global climate (Charlson et al., 1987; Yu et al., 2007; Menon et al., 2002; Houghton et al., 2001). Megacities play a particular role in this regard. They comprise a significant source for anthropogenic aerosol particles (Alpert et al., 2012; Cassiani et al., 2013), therefore, they are of interest in global climate and chemical models (Lawrence et al., 2007; Butler and Lawrence, 2009; Folberth et al., 2012). Trends of anthropogenic aerosol particles over the 189 largest cities in the world were reported by Alpert et al. (2012) utilizing data products of three satellite sensors.

One measure to describe the extinction (absorption plus scattering) of solar radiation by aerosol particles is the aerosol optical depth (AOD). It can be measured from the ground by Sun photometers or retrieved by measurements of upward radiances taken from spaceborne instruments such as the MODerate resolution Imaging Spectroradiometer (MODIS) (Schaaf et al., 2002). The measured upward radiance at the top of atmosphere (TOA) is affected by both, the reflection due to atmospheric components and the underlying surface. The AOD retrieval uncertainty mainly depends on surface reflectance assumptions for a low aerosol ( $AOD < 0.15$ ), whereas aerosol model assumptions are crucial for  $AOD > 0.4$  (Levy et al., 2010; Mielonen et al., 2011). In general the AOD retrieval over dark surfaces (as ocean water) involves lower uncertainties than results obtained above land (Kaufman et al., 1997). Collections 5 (C5) and C6 of the MODIS algorithm for the AOD retrieval over land use the dark-target method to isolate the surface contribution in the measured TOA reflectance (Levy et al., 2007, 2010, 2013). In C5 and C6 the different spectral dependencies of the surface reflectance are taken into account by a vegetation index which slightly modifies the surface assumptions in the algorithm. However, the algorithm developed for dense dark vegetation shows lower performance for urban surfaces (de Almeida Castanho et al., 2007; Oo

# AMTD

8, 7335–7371, 2015

## Adaption of the MODIS aerosol retrieval algorithm

E. Jäkel et al.

Title Page

Abstract

Introduction

Conclusions

References

Tables

Figures



Back

Close

Full Screen / Esc

Printer-friendly Version

Interactive Discussion



et al., 2010; Wong et al., 2011; Zha et al., 2011; Li et al., 2012; Escribano et al., 2014), or surfaces with high reflectance such as arid regions (Drury et al., 2008). Specifically, as found by de Almeida Castanho et al. (2007) and Oo et al. (2010), C5 data showed a positive bias of retrieved AOD over Mexico City and New York City compared to ground-based Sun photometer measurements.

Several approaches have been suggested to consider the problem of unknown surface reflectance in the retrieval of AOD from MODIS data. Drury et al. (2008) found an improvement of the derived AOD if the local surface reflectance was used as derived from satellite data for days of low AOD. Furthermore, the application of a chemical transport model for the aerosol properties improved the AOD retrieval. Wong et al. (2011) developed an aerosol retrieval algorithm for Hong Kong and the Pearl River Delta region with a spatial resolution of 500 m. They determined the surface reflectance with a minimum reflectance technique which increased the slope of the linear regression coefficient between AODs from MODIS and Sun photometer measurements from 0.75 to 0.83. A simplified algorithm to retrieve AODs with a spatial resolution of 500 m for urban regions such as Beijing was developed by Bilal et al. (2014). The results have shown a relative mean bias (RMB, ratio of AOD from MODIS and AOD derived from Sun photometer at “Beijing\_RAD1” AERONET site) of 0.97, whereas the standard MODIS algorithm overestimated the AOD with a RMB of 1.12. Zha et al. (2011) used Sun photometer measurements and radiative transfer calculations for an improved representation of surface reflectance in the MODIS algorithm. They have shown for the city of Nanjing, China, a seasonal variability of the relationship between the surface reflectance at the visible (0.47 and 0.65  $\mu\text{m}$ ) and the near infrared wavelengths (2.11  $\mu\text{m}$ ).

The present study focuses on the sensitivity of the operational MODIS aerosol algorithms (C5 and C6) over land with respect to surface reflectance assumptions over densely populated, urban areas. In contrast to previous investigations using the standard MODIS AOD retrieval this study utilized surface reflectances derived from airborne spectral measurements (taken over Zhongshan, Southeast China). The outline of this study is as follows:

## Adaption of the MODIS aerosol retrieval algorithm

E. Jäkel et al.

Title Page

Abstract

Introduction

Conclusions

References

Tables

Figures



Back

Close

Full Screen / Esc

Printer-friendly Version

Interactive Discussion





## Adaption of the MODIS aerosol retrieval algorithm

E. Jäkel et al.

Title Page

Abstract

Introduction

Conclusions

References

Tables

Figures

◀

▶

◀

▶

Back

Close

Full Screen / Esc

Printer-friendly Version

Interactive Discussion



and the remaining pixels are checked with respect to their brightness. For that purpose only pixels with reflectances between 0.01 and 0.25 at 2.11  $\mu\text{m}$  wavelength are selected. The brightest 50 % and darkest 20 % of these pixels are discarded in order to further reduce possible cloud and surface contamination. If there are at least 12 remaining pixels within the 10 km by 10 km box, the reflectance in each channel is averaged and taken to represent the TOA reflectance of this box.

C6 provides also an aerosol data product with 3 km resolution using different pixel selections but only as a subset of the standard 10 km resolution data set. The spectral surface reflectance cannot be determined directly from satellite measurements. The MODIS AOD algorithms use assumptions according to the spectral reflectance over land on dense dark vegetation. For Collection 4 (C4) Kaufman et al. (1997) determined that for vegetated and dark-soiled surfaces, the surface reflectances in blue (0.49  $\mu\text{m}$ ), red (0.66  $\mu\text{m}$ ) and in the near infrared (2.1  $\mu\text{m}$ ) can be related by empirical relationships:  $\rho_{0.49} = \rho_{2.1}/4$  and  $\rho_{0.66} = \rho_{2.1}/2$ . Furthermore, except for dust or heavy aerosol, the atmosphere is nearly transparent at 2.1  $\mu\text{m}$ , so that the surface reflectance ( $\rho_{s,2.1}$ ) is about the reflectance at TOA ( $\rho_{\text{TOA},2.1}$ ). Therefore, the aerosol retrieval could be constrained by the surface reflectance relationships, in that the difference between TOA and surface in blue and red channels can be related to aerosol. C5 and C6 consider more flexible assumptions in terms of the wavelength-dependent surface reflectance. Levy et al. (2007) noted that the surface spectral relationships are also function of scattering angle  $\vartheta_{\text{scat}}$  and general “greenness” of the surface, and revised the empirical relationships in C5 and C6. The effect of geographical and seasonal variations on surface properties in terms of vegetation could be diagnosed through the use of the normalized differenced vegetation index  $\text{NDVI}_{\text{SWIR}}$ :

$$\text{NDVI}_{\text{SWIR}} = \frac{\rho_{1.2}^{\text{m}} - \rho_{2.1}^{\text{m}}}{\rho_{1.2}^{\text{m}} + \rho_{2.1}^{\text{m}}}. \quad (1)$$

The surface reflectance at 2.1  $\mu\text{m}$  wavelength is calculated as a function of measured TOA reflectance, the atmospheric backscatter ratio, the transmissivity, and the TOA

reflectance given by the precalculated Look-Up Tables (LUT) depending on AOD and aerosol type. Based on the surface reflectance at 2.1  $\mu\text{m}$  wavelength, the surface reflectance at 0.65 and 0.47  $\mu\text{m}$  is derived by:

$$\rho_{s,0.65} = \rho_{s,2.1} \cdot a_{0.65/2.1} + b_{0.65/2.1}, \quad (2)$$

$$5 \quad \rho_{s,0.47} = \rho_{s,0.65} \cdot a_{0.47/0.65} + b_{0.47/0.65}. \quad (3)$$

The corresponding slopes  $a$  and intercepts  $b$  are given by:

$$a_{0.65/2.1} = a_{0.65/2.1}^{\text{NDVI}} + 0.002 \cdot \vartheta_{\text{scat}} - 0.27,$$

$$b_{0.65/2.1} = -0.00025 \cdot \vartheta_{\text{scat}} + 0.033,$$

$$a_{0.47/0.65} = 0.49,$$

$$10 \quad b_{0.47/0.65} = 0.005, \quad (4)$$

with the scattering angle  $\vartheta_{\text{scat}}$  and the slope  $a_{0.65/2.1}^{\text{NDVI}_{\text{SWIR}}}$  is chosen with respect to the vegetation index  $\text{NDVI}_{\text{SWIR}}$ . Note, that due a coding error in C5 the  $\text{NDVI}_{\text{SWIR}}$  dependencies were reversed in C6 (Levy et al., 2013):

$$a_{0.65/2.1}^{\text{NDVI}} = 0.48 \quad (\text{C5}) \quad \text{and} \quad a_{0.65/2.1}^{\text{NDVI}} = 0.58 \quad (\text{C6}) \quad \text{for: } \text{NDVI} < 0.25, \quad (5)$$

$$15 \quad a_{0.65/2.1}^{\text{NDVI}} = 0.58 \quad (\text{C5}) \quad \text{and} \quad a_{0.65/2.1}^{\text{NDVI}} = 0.48 \quad (\text{C6}) \quad \text{for: } \text{NDVI} > 0.75, \quad (6)$$

$$a_{0.65/2.1}^{\text{NDVI}} = 0.48 + 0.2 \cdot (\text{NDVI} - 0.25) \quad (\text{C5}) \quad \text{and}$$

$$a_{0.65/2.1}^{\text{NDVI}} = 0.58 + 0.2 \cdot (\text{NDVI} - 0.25) \quad (\text{C6}) \quad \text{for: } 0.25 \leq \text{NDVI} \leq 0.75. \quad (7)$$

For the sensitivity studies presented in the following sections the standalone codes of the MODIS aerosol retrieval algorithms over land of C5 and C6 were applied (<http://darktarget.gsfc.nasa.gov/reference/code>). These codes provide a single output AOD for a given set of input values. All assumptions about pixel aggregation, cloud masking and pixel selection have already been applied prior to the standalone code and is not part of this study.

## Adaption of the MODIS aerosol retrieval algorithm

E. Jäkel et al.

Title Page

Abstract

Introduction

Conclusions

References

Tables

Figures



Back

Close

Full Screen / Esc

Printer-friendly Version

Interactive Discussion



## 2.2 Airborne measurements of urban surface reflection properties

The aerosol MODIS standard retrieval will be modified by changes of the assumptions of the surface reflectances using airborne measurements carried out over Zhongshan, China. The following subsection introduces the field campaign, the main instruments, and the method to retrieve the surface properties.

### 2.2.1 Field campaign in Zhongshan, Pearl River Delta, China

In December 2009 airborne measurements of solar radiation reflected by the surface were performed over the densely populated urban region of Zhongshan, China. The city of Zhongshan was chosen due to its location in the vicinity of the megacities Guangzhou, Shenzhen, and Hong Kong. This area is characterized by a distinct heterogeneous urban surface reflectance pattern including various artificial materials as well as vegetation and small water bodies, and a usually high aerosol load. Spectral solar radiation was measured with the Spectral Modular Airborne Radiation measurement system albedometer (SMART albedometer, Wendisch et al., 2001, 2004; Bierwirth et al., 2009). During the campaign the instrument was equipped with two kinds of optical inlets, one for spectral upward irradiance ( $F_{\lambda}^{\uparrow}$ ), the other for spectral nadir radiance ( $I_{\lambda}^{\uparrow}$ ) measurements (opening angle of radiance inlet =  $2.1^{\circ}$ ). Each optical inlet was connected via optical fibers to two multichannel spectrometers. The spectrometers cover a wavelength range between 0.4–2.1  $\mu\text{m}$  with a full width at half maximum (FWHM) of 1–2 and 9–16 nm, respectively. The reliable spectral range depends on the sensitivity of the spectrometers. Due to low signal and poor sensitivity only nadir radiances below 2.0  $\mu\text{m}$  are used in this study. Laboratory calibrations with certified radiation sources (1000 W lamp, integrating sphere, and Lambert reflecting panel) prior and after the field campaign, as well as field calibrations during the campaign were carried out to calculate the radiation quantities from the raw signal. The measurement uncertainty of the SMART albedometer includes calibration lamp and transfer calibration uncertainties as well as the wavelength accuracy of the spectrometers. This results in a total

## Adaption of the MODIS aerosol retrieval algorithm

E. Jäkel et al.

Title Page

Abstract

Introduction

Conclusions

References

Tables

Figures



Back

Close

Full Screen / Esc

Printer-friendly Version

Interactive Discussion



spectral dependent uncertainty ranging from 3 to 14 %, calculated with Gaussian error propagation.

Concurrently, ground-based data of aerosol properties were collected in the city of Zhongshan with two Sun photometers (Cimel CE318-2 and Schulz SP1A) and a LIDAR as presented in Chen et al. (2014). From these data the single scattering albedo  $\tilde{\omega}$  and asymmetry parameter  $g$  of the aerosol particles were retrieved by the inversion method described by Dubovik and King (2000). The vertical aerosol extinction profile  $b_{\text{ext}}(z)$  was measured with a combined Raman (387 nm), elastic (355 and 532 nm) backscatter LIDAR. An overview of all airborne and ground-based instruments, as well as their measurement uncertainties are given in Table 1 (after Andrews et al., 2006; Chen et al., 2014).

The measured data from the Sun photometers and LIDAR were used to describe the spectral vertical extinction profile which is needed for the calculation of surface reflectance and surface albedo from the airborne radiance and irradiance measurements by excluding the atmospheric masking (see Sect. 2.3). Since no information on the vertical aerosol distribution is available up to 1000 m height, the vertical extinction profile was extrapolated to the surface using two layers with a different vertical distribution of the extinction. Starting from 1000 m altitude the extinction initially increases with decreasing height following the measured slope of the LIDAR above 1000 m. A second layer with a vertically homogeneous extinction coefficient is assumed below representing a well-mixed layer. The vertical dimension of both layers was chosen so that the vertically integrated extinction coefficient corresponds with the measured AOD of the Sun photometer. The Sun photometer measurements of AOD,  $\tilde{\omega}$ ,  $g$  were extrapolated to wavelengths larger than 1  $\mu\text{m}$  by scaling spectra from the literature (d'Almeida et al., 1991).  $\tilde{\omega}$  and  $g$ , were assumed to be constant with height. For the AOD it was assumed that the shape of the vertical profile has no spectral dependence. In this way the extinction profile was scaled with the spectral Sun photometer AOD measurements to obtain extinction profiles at different wavelengths.

## Adaption of the MODIS aerosol retrieval algorithm

E. Jäkel et al.

[Title Page](#)[Abstract](#)[Introduction](#)[Conclusions](#)[References](#)[Tables](#)[Figures](#)[Back](#)[Close](#)[Full Screen / Esc](#)[Printer-friendly Version](#)[Interactive Discussion](#)

## 2.3 Retrieval of surface reflectance and albedo from airborne measurements

The spectral surface reflectance  $\rho_{s,\lambda}$  was calculated according to the atmospheric correction technique described by Wendisch et al. (2004). This method to remove the atmospheric masking was originally developed for the retrieval of the surface albedo  $\alpha_{s,\lambda}$  based on airborne measured irradiance. Note, that Wendisch et al. (2004) used the symbol  $\rho_s$  for the surface albedo. Atmospheric masking means that a downward-looking radiation sensor measures not only the contribution of reflected radiation from the surface but is also influenced by the multiple scattering within the atmosphere, which needs to be separated. The surface reflectance

$$\rho_{s,\lambda} = \frac{\pi \cdot I_{\lambda}^{\uparrow}(z_0)}{F_{\lambda}^{\downarrow}(z_0)} \quad (8)$$

is retrieved by assuming isotropic surface reflectance with  $F = \pi \cdot I$ . Both surface properties are obtained by an iterative algorithm starting with an initial value of albedo (reflectance) at flight level  $\alpha_m(z_F)$  [ $\rho_m(z_F)$ ], which is used as a first guess for the surface albedo (reflectance). The spectral upward irradiance and radiance as well as the spectral downward irradiance at flight level  $z_F$  and at ground level  $z_0$  are calculated with the one-dimensional radiative transfer package libRadtran (Mayer and Kylling, 2005). The Sun photometer and LIDAR measurements provide the input for the aerosol profile as described above. Furthermore, the model uses atmospheric profiles of temperature, pressure, and gas concentrations. The simulated albedo (reflectance) at flight level and ground level is used to calculate the surface albedo (reflectance) for the next iteration step  $\alpha_{n+1}$  ( $\rho_{n+1}$ ) as follows:

$$\alpha_{n+1}(z_0) = \alpha_m(z_F) \cdot \frac{\alpha_n(z_0)}{\alpha_n(z_F)} \quad (9)$$

$$\rho_{n+1}(z_0) = \rho_m(z_F) \cdot \frac{\rho_n(z_0)}{\rho_n(z_F)} \quad (10)$$

The iteration is stopped if the difference between measured  $F_m^\uparrow$  ( $I_m^\uparrow$ ) and modeled upward irradiance  $F_{n+1}^\uparrow$  (radiance  $I_{n+1}^\uparrow$ ) is less than 4 % (6 %) which is comparable to the measurement uncertainty of the upward irradiance (radiance):

$$\left| \frac{F_{n+1}^\uparrow(z_F)}{F_m^\uparrow(z_F)} - 1 \right| \leq 0.04 \quad (11)$$

$$\left| \frac{I_{n+1}^\uparrow(z_F)}{I_m^\uparrow(z_F)} - 1 \right| \leq 0.06. \quad (12)$$

The uncertainties of the retrieved surface albedo and reflectance were determined by Gaussian error propagation of the single error sources (see Table 2). For this purpose a sensitivity study with radiative transfer calculations was performed. Synthetic upward radiances and irradiances at a given flight altitude  $z_F$  were calculated with one-dimensional radiative transfer calculations for given aerosol and surface albedo input. Afterwards the surface albedo and surface reflectance was determined with the method described above, first for the given input values, and subsequently with modified input parameters. The variations of the single aerosol parameters were: AOD  $\pm 30\%$ ,  $\tilde{\omega} \pm 2$ ,  $g \pm 4\%$ , and  $z_F \pm 50$  m. These uncertainties were assumed from the observed variation of the parameters during the field campaign in Zhongshan. The variation of  $F_\lambda^\uparrow$  and  $I_\lambda^\uparrow$  were  $\pm(3\text{--}14)\%$  dependent on the considered wavelength range according to the measurement uncertainties. Especially for the wavelength range of 0.4–0.6  $\mu\text{m}$  the estimated total uncertainty of surface albedo and surface reflectance yields values of 36 and 18 %, demonstrating the high sensitivity to the optical aerosol properties. For increasing wavelength this sensitivity decreases because of the decrease of the AOD for higher wavelength. Consequently, also the sensitivity of single scattering albedo and asymmetry parameter is enhanced for shorter wavelengths. For larger wavelengths the

## Adaption of the MODIS aerosol retrieval algorithm

E. Jäkel et al.

Title Page

Abstract

Introduction

Conclusions

References

Tables

Figures



Back

Close

Full Screen / Esc

Printer-friendly Version

Interactive Discussion



total uncertainty is mainly dominated from the measurement uncertainty of SMART, which has lower sensitivity and poor signal-to-noise-ratio in this spectral range.

### 3 Results from airborne measurements

#### 3.1 Example spectra of surface reflectance and albedo

5 An area of 8 km by 4 km of the city of Zhongshan was systematically overflown on 03 December 2009, with  $60 \text{ m s}^{-1}$  flight speed in different altitudes as shown in Fig. 1. The upward radiances and irradiances measured within the marked area are used to calculate the surface albedo and surface reflectance spectra. As an example, mea-  
10 surements at 4100 m flight altitude correspond to a radiance footprint of 140 m across and 200–380 m along the flight direction for each measurement depending on the chosen integration time of the SMART-Albedometer with an radiance inlet opening angle of  $2.1^\circ$ . The solar zenith angle  $\theta_0$  ranged between  $44$  and  $55^\circ$  during the 1.5 h of the flight. The change of the solar zenith angle (SZA) was considered in the derivation of the surface properties.

15 Typical examples of spatially-averaged surface albedo and reflectance spectra derived from the airborne measurements in 4100 m altitude over Zhongshan are presented in Fig. 2. Note, that significant absorption bands are excluded. The corresponding standard deviation, displayed as vertical bars, represents a measure of the heterogeneity of the underlying urban surface. Both spectra in Fig. 2 show spectral signatures  
20 typical for vegetation. Especially the vegetation step, a strong increase of albedo or reflectance in the range of  $0.7\text{--}0.9 \mu\text{m}$ , is obvious. The surface albedo is lower than the surface reflectance for all wavelengths which mainly depends on the bidirectional reflection of the underlying surface, the solar zenith and azimuth angles during the measurements. The standard deviation of the spatially-averaged surface albedo, derived  
25 from measurements in 4100 m flight altitude is smaller than that of the concurrently measured surface reflectance. This can be explained by the definition of albedo as the

## Adaption of the MODIS aerosol retrieval algorithm

E. Jäkel et al.

Title Page

Abstract

Introduction

Conclusions

References

Tables

Figures



Back

Close

Full Screen / Esc

Printer-friendly Version

Interactive Discussion



ratio of the upward and downward irradiance. Irradiances are related to radiation entering from the entire hemisphere (cosine weighted). Therefore, the variability of the retrieved spatially-averaged surface albedo from airborne measurements strongly depends on the flight altitude but also on aerosol conditions (Jäkel et al., 2013). Resolving the small-scale variability of surface albedo would require very low-flying aircraft or ground-based measurements. The surface reflectance derived from radiance measurements at high flight altitudes, on the other hand, still reproduces the heterogeneity of the surface reflection caused by the narrow viewing angle of the radiance optical inlet.

### 3.2 New surface reflectance assumptions for the MODIS AOD retrieval method

According to Eqs. (2) and (3) the surface reflectance at  $0.47\ \mu\text{m}$  wavelength in the MODIS AOD algorithm is derived from that at  $0.65\ \mu\text{m}$  based on the surface reflectance at  $2.1\ \mu\text{m}$ . Since the airborne measurements of the surface reflectance are not reliable above  $2.0\ \mu\text{m}$  spectral range due to poor sensitivity and low signal, here only the fit parameter of Eq. (3) in the C5 and C6 code will be adapted by the results taken from the Zhongshan data set. The variability of the urban surface reflectance and surface albedo as indicated by the vertical bars in Fig. 2 induces a more surface dependent treatment of the surface reflectance within the AOD retrieval. The surface reflectance at  $0.47\ \mu\text{m}$  as function of the surface reflectance at  $0.65\ \mu\text{m}$  for the case study Zhongshan is shown in Fig. 3a. To compare the assumed correlation used in the operational MODIS algorithm (dashed line) and the measured correlation we performed a linear regression with an intercept and a slope parameter (red solid line):

$$\rho_{s,0.47} = 0.005 + 0.49 \cdot \rho_{s,0.65} \quad \text{MODIS – operational,} \quad (13)$$

$$\rho_{s,0.47} = 0.02 + 0.63 \cdot \rho_{s,0.65} \quad \text{Zhongshan; regression with intercept.} \quad (14)$$

Equations (13) and (14) reveal a systematic bias between both regression. In Sect. 4 the effect of the surface property variation on the retrieved AOD will be discussed.

## Adaption of the MODIS aerosol retrieval algorithm

E. Jäkel et al.

Title Page

Abstract

Introduction

Conclusions

References

Tables

Figures

◀

▶

◀

▶

Back

Close

Full Screen / Esc

Printer-friendly Version

Interactive Discussion





## 4.1 Implementation of measured surface reflectance ratios into the MODIS algorithm

Satellite measurements of the reflectance at TOA from the MODIS products MOD04 (from Terra satellite) and MYD04 (from Aqua satellite) were used as input for the standalone code of the operational aerosol retrieval. This data is already cloud screened and averaged to 10 km by 10 km pixels. For improved comparability between the adapted and original slope assumptions in C5 and C6, the standalone code was applied for reflectance data as given in the C5 product. So differences in the derived AOD are solely caused by the modification of the standalone code, not by differences in the preprocessing of the data between C5 and C6. Data and pixel were chosen to fit the time and area of the airborne measurements as best as possible in order to minimize differences due to season and viewing geometry. Therefore, the MODIS aerosol product from 01 December 2009, was used as optimum choice with respect to observed location and solar geometry ( $SZA = 45.7^\circ$ ). No Sun photometer measurements were available on this day to compare the results of this sensitivity study with ground-based AOD data. Figure 4a shows the retrieved AOD ( $0.55 \mu\text{m}$ ) as function of the spectral slope  $a_{0.47/0.65}$  measured in Zhongshan for the modified C5 and C6 retrieval. For this range of spectral slopes an almost linear relationship between slope and retrieved AOD is observed with a correlation coefficient of 0.99 for both algorithms. In this particular case a spectral slope between 0.55 and 1.10 results in an AOD ranging between 0.75 and 0.87. Here, C6 tends to a slightly lower AOD for larger slopes compared to C5. Figure 4b shows the relative frequency distribution of AOD ( $0.55 \mu\text{m}$ ) as retrieved with the MODIS C5 and C6 algorithm using the whole variation of the slope parameter  $a_{0.47/0.65}$  (Fig. 3). The AOD values of 0.84 (C5) and 0.85 (C6) as retrieved by the original MODIS algorithms are displayed as vertical lines. In most of the cases the modified algorithms yielded values (mean values of AOD for C5:  $0.83 \pm 0.02$  and C6:  $0.82 \pm 0.02$ ) lower than the operational MODIS algorithms caused by a different assumed correlation between the reflectances of 0.47 and 0.65  $\mu\text{m}$  (see Eq. 13).

## Adaption of the MODIS aerosol retrieval algorithm

E. Jäkel et al.

Title Page

Abstract

Introduction

Conclusions

References

Tables

Figures



Back

Close

Full Screen / Esc

Printer-friendly Version

Interactive Discussion



In a next step the slopes  $a_{0.47/0.65}$  derived from measurements over Zhongshan were applied on MODIS data for a different urban area (Beijing) where AERONET data are available for several years. The MODIS data (MOD04) of the years 2010–2014 were filtered with respect to season (April–September) to take into account the vegetation period similar to that in the Zhongshan data (subtropical region). Furthermore, the viewing sensor zenith angle was restricted to a range of 0 to 10° which is comparable with the range observed during the aircraft measurements of the reflectance ratios over Zhongshan. A number of 21 cases for the immediate surrounding of the AERONET station Beijing were found. As for Zhongshan the operational and the modified C5 and C6 algorithms were applied to these data.

Figure 5 presents the difference of the derived AOD from AOD(AERONET) as a function of the AOD(AERONET). A systematic overestimation is obvious for the operational C5 (mean AOD =  $0.31 \pm 0.11$ ) and C6 method (mean AOD =  $0.18 \pm 0.12$ ). The operational code assumes a dark surface, so that a larger reflectance will be interpreted as enhanced reflectance contribution due to a higher aerosol load. However, the operational C6 method shows an improved agreement with AERONET data compared to C5. Using the measured  $a_{0.47/0.65}$ -spectral slopes in C5 and C6 reveals lower AOD values compared to the retrieved AOD values of the operational algorithms. For the modified C5 method we can observe a significantly improvement of the agreement between AOD(AERONET) and AOD(MODIS) (mean AOD =  $0.09 \pm 0.18$ ). However, the modified C6 method underestimates the retrieved AOD (mean AOD =  $-0.10 \pm 0.18$ ). In particular for lower AOD values ( $\leq 0.35$ ) also negative AOD values are derived. Despite a lower absolute mean difference to AOD(AERONET) than the operational methods, the modified C6 method shows a poor performance compared to the other methods.

As can be seen from Fig. 5 the mean difference of the modified algorithms and AERONET data is lower than for the operational methods. However, the AOD standard deviations have increased (from  $\pm 0.10$  to  $\pm 0.18$ ) with the adapted algorithms. The reason might be the different correlation between the reflectance at TOA and AOD. For dark surfaces (as assumed in the operational retrieval) the increase of reflectance at

TOA with AOD is larger than for bright surfaces. Consequently, measurement uncertainties have larger effects on data over brighter surfaces.

Bilal et al. (2014) have applied their approach to Beijing data for 2012 and 2013. Their method includes revised assumptions of the surface reflection but also changes in the aerosol model that uses AERONET data of  $\tilde{\omega}$  nad  $g$ . Bilal et al. (2014) achieved a correlation with AERONET data with a coefficient of correlation of 0.95 and a relative mean bias of 0.97 [AOD(retrieved)/AOD(AERONET)]. For the modified C5 algorithm a correlation coefficient of 0.92 and a relative mean bias of 1.08 was derived (cf. operational C5: correlation coefficient = 0.93, relative mean bias = 1.68, operational C6: correlation coefficient = 0.90, relative mean bias = 1.46). In Fig. 5 only the mean values of the retrieved AOD-distributions derived from the adapted methods are used. The spread of the AOD distributions depend significantly on the AOD, higher values of AOD lead to a smaller spread of retrieved AODs (standard deviation = 0.03 for AOD = 1.6 vs. standard deviation = 0.18 for AOD = 0.2) which demonstrates the decreasing sensitivity of the spectral surface reflection assumptions on the retrieval uncertainty with increasing AOD as already shown by Levy et al. (2010) and Mielonen et al. (2011).

For further interpretation the areal distribution of the AOD (contour lines) over Beijing (17 May 2012) retrieved from MODIS measurements by the operational and adapted C5 and C6 methods are presented in Fig. 6. A map of the area to illustrate the distribution of urban and rural areas is plotted behind the AOD data. The AERONET station has measured an AOD of 0.55 for the time of the satellite overpass. The operational algorithms C5 and C6 have shown AODs of about 0.8 (C5) and 0.7 (C6) over Beijing (116.381° N, 39.977° E). By applying the modified algorithms the AODs over Beijing decreased to values of 0.5 (C5) and 0.28 (C6). For rural areas the modified methods fail to retrieve the AOD. There, negative values are derived which are excluded from the contour plots in Fig. 6. However, as shown in this example, for urban areas the modified algorithm (C5 in particular) improves the agreement between AERONET and MODIS AOD.

Adaption of the  
MODIS aerosol  
retrieval algorithm

E. Jäkel et al.

Title Page

Abstract

Introduction

Conclusions

References

Tables

Figures



Back

Close

Full Screen / Esc

Printer-friendly Version

Interactive Discussion



## 4.2 Sensitivity study of the VIS-to-NIR reflectance ratios

According to Eq. (2) the MODIS AOD retrieval also considers the surface reflectance at  $2.1\ \mu\text{m}$  which cannot be deduced from the airborne measurements due to a lack of sensitivity for wavelengths larger than  $2.0\ \mu\text{m}$ . In order to account for the surface reflectance at  $2.1\ \mu\text{m}$  and its relation to that at  $0.65\ \mu\text{m}$  a sensitivity study based on radiative transfer simulations was performed. Simulated reflectances at TOA for variable surface properties (surface albedo) have been used to generate synthetic MODIS measurements providing the input for the AOD retrieval. The spectral slope and y-intercept for the calculation of  $\rho_{0.65}$  and  $\rho_{0.47}$  (Eq. 3) in the standalone code of the aerosol retrieval over land were modified according to the spectra of the different surface types used for the simulation of the TOA reflectances. Figure 7a shows the four surface albedo spectra of the different surface types (Kentucky Bluegrass, Bowker et al., 1985, Oasis and Farmland, Bierwirth et al., 2009, and urban, measurements over Zhongshan) for the wavelength range of  $0.4\text{--}2.1\ \mu\text{m}$ . All data were derived from aircraft irradiance measurements. Note, that the raw signal of the irradiance is higher than for the radiance measurements. Therefore, reliable data can be given up to a wavelength of  $2.1\ \mu\text{m}$ . The gaps indicate absorption bands; they are excluded when deducing the surface albedo from airborne measurements following the procedure described in Sect. 2. A strong increase of surface albedo at  $0.7\ \mu\text{m}$  due to vegetation is typical for the surface types Kentucky Bluegrass (gray dots) and Oasis (red dots). Also for the urban surface type a small increase, indicating the impact of vegetation, is visible, but less prominent in comparison to Kentucky Bluegrass and Oasis. The surface albedo spectrum of Farmland shows the highest albedo values for wavelengths below  $0.7\ \mu\text{m}$  and differs most compared to the spectrum of Kentucky Bluegrass.

The spectral characteristic of the optical properties of the aerosol particles, as used in the simulation of reflectances at TOA, are presented in Fig. 7b. For a wavelength of  $0.55\ \mu\text{m}$  the AOD was set to 0.85 which is comparable to the aerosol conditions during the measurement campaign in Zhongshan. Values of  $\tilde{\omega}(0.55\ \mu\text{m}) = 0.9$  and  $g(0.55\ \mu\text{m})$

### Adaption of the MODIS aerosol retrieval algorithm

E. Jäkel et al.

[Title Page](#)[Abstract](#)[Introduction](#)[Conclusions](#)[References](#)[Tables](#)[Figures](#)[Back](#)[Close](#)[Full Screen / Esc](#)[Printer-friendly Version](#)[Interactive Discussion](#)

## Adaption of the MODIS aerosol retrieval algorithm

E. Jäkel et al.

Title Page

Abstract

Introduction

Conclusions

References

Tables

Figures



Back

Close

Full Screen / Esc

Printer-friendly Version

Interactive Discussion



= 0.7 were applied according to the Sun photometer measurements in Zhongshan. The aerosol particles are more absorbing than the moderately absorbing aerosol type [ $\tilde{\omega}(0.55 \mu\text{m}) = 0.92$ ] in the MODIS algorithm, but less absorbing than the absorbing aerosol type [ $\tilde{\omega}(0.55 \mu\text{m}) = 0.87$ ]. The asymmetry parameter used for the simulations in this study compares with the spheroid dust model [ $g(0.55 \mu\text{m}) = 0.7$ ] and the weak absorbing aerosol type [ $g(0.55 \mu\text{m}) = 0.68$ ].

First, the AOD for each surface type was retrieved with the operational algorithm. Then the spectral slopes  $a_{0.65/2.1}$  and  $a_{0.47/0.65}$  were adapted for each surface type which gives four specific slopes corresponding to the surface type. The y-intercepts  $b_{0.65/2.1}$  and  $b_{0.47/0.65}$  were set to zero, because only one spectrum for each surface type was used. An overview of the slopes and y-intercepts used by the operational algorithm and those obtained from the example spectra are presented in Table 3. In most of the cases the slopes  $0.43 \leq a_{0.47/0.65} \leq 1.0$  and  $0.30 \leq a_{0.65/2.1} \leq 0.8$  valid for the different surface types differ from those used in the operational algorithm ( $a_{0.47/0.65} = 0.49$  and  $0.48 \leq a_{0.65/2.1} \leq 0.59$ ). The AOD results of the four algorithms for all surface types are listed in Table 4. Best agreement of the operational algorithm C5 (C6) with the input value of  $\text{AOD}(0.55 \mu\text{m}) = 0.85$  was found for underlying dark vegetated surfaces with  $\text{AOD}(0.55 \mu\text{m}) = 0.87$  (0.88) for the case of Kentucky Bluegrass and  $\text{AOD}(0.55 \mu\text{m}) = 0.85$  (0.86) for the Oasis surface type. The worst performance of the operational algorithms was obtained for the Farmland and the Urban surface type. While for the Urban surface an overestimation of the AOD was observed with a relative mean bias of 16 and 19%, which confirms the outcome of the Beijing – study in Sect. 4.1, the retrieved AOD for the Farmland surface type is significantly underestimated (C6 with  $\text{RMB} = 70\%$ ). Both algorithms C5 and C6 include a threshold for their brightness criteria ( $2.1 \mu\text{m}$  reflectance  $> 0.25$ ) which is exceeded for the farmland case ( $2.1 \mu\text{m}$  reflectance = 0.26). As stated by Levy et al. (2010) the retrieval is error-prone for cases above the brightness criteria. This underestimation can also be found in the modified algorithms with surface adapted slopes. This also indicates the increased un-

certainty for data which exceed the brightness criteria. For all other surfaces (Kentucky Bluegrass, Oasis, and Urban) the modified algorithms exhibit good performances.

## 5 Conclusions

Uncertainties of the operational MODIS AOD algorithms Collections 5 and 6 over the densely populated urban area of Zhongshan and Beijing, China, have been quantified. The retrieved AOD significantly depends on surface reflectance assumptions within the retrieval algorithms which often show a positive bias of retrieved AOD over urban areas. This issue was investigated twofold. First, surface reflectance assumptions were modified in the standard algorithms C5 and C6 using airborne measurements of surface reflectance over Zhongshan. These assumptions consider spectral relationships between the surface reflectance at  $0.47\ \mu\text{m}$  and at  $0.65\ \mu\text{m}$ . The modified retrieval methods have been applied to MODIS measurements taken during the aircraft campaign in the Zhongshan area. Additionally, the AOD retrieved by the standard and modified algorithms based on MODIS measurements from 2010 to 2014 over Beijing have been compared with AERONET. In a second approach the sensitivity of the AOD retrieval for several surface types was studied using synthetic MODIS data obtained from radiative transfer simulations.

Specifically, airborne measurements of the spectral nadir radiance have been used to retrieve the spectral surface reflectance using aerosol properties obtained from Sun photometer and LIDAR of the Zhongshan area. The fit parameters of the linear relationship between the surface reflectance at  $0.47\ \mu\text{m}$  and at  $0.65\ \mu\text{m}$  in C5 and C6 were varied based on the variability of the measured reflectances over Zhongshan. Due to a lack of sensitivity and a low raw signal above of  $2.0\ \mu\text{m}$  wavelength of the airborne instrument SMART albedometer (radiance component) only the  $a_{0.47/0.65}$  slopes were modified in C5 and C6. The distribution of  $a_{0.47/0.65}$  slopes over Zhongshan has revealed a mean value of  $0.85 \pm 0.09$ . This indicates a less spectral dependence of the

## Adaption of the MODIS aerosol retrieval algorithm

E. Jäkel et al.

Title Page

Abstract

Introduction

Conclusions

References

Tables

Figures



Back

Close

Full Screen / Esc

Printer-friendly Version

Interactive Discussion



surface reflectance over urban areas in the visible spectral range than assumed in the operational algorithm where a fixed spectral slope of 0.49 is used.

For the measurement case over Zhongshan the standard retrievals [AOD = 0.84 (C5) and AOD = 0.85 (C6)] show only a low positive bias compared to the AOD retrieval by the modified algorithms [ $0.83 \pm 0.02$  (C5) and  $0.82 \pm 0.02$  (C6)] which is within the measurement uncertainty. Since no AERONET data were available for Zhongshan we applied the modified AOD retrievals for MODIS data over Beijing for a period of 2010 to 2014. While the operational algorithms C5 and C6 have shown a significant positive bias compared to AERONET with a mean difference of 0.31 and 0.18, the modified C5 algorithm revealed a mean difference of 0.09. An application of the adapted methods with urban surface reflection assumptions for non-urban surfaces resulted in negative AOD values. Therefore, the adapted methods are only recommended for large urban areas, because the spatial resolution of the MODIS product is 10 km. A mixture of urban and vegetated surfaces would allow the agreement to ground-based photometer measurements.

The sensitivity study based on radiative transfer simulations of the reflectance at TOA (representing MODIS measurements) for given conditions as surface and aerosol properties, confirmed that both operational MODIS aerosol retrievals (C5 and C6) over land can reproduce the input AOD( $0.55 \mu\text{m}$ ) of 0.85 for the surface types Kentucky Bluegrass [AOD( $0.55 \mu\text{m}$ ) = 0.87 (C5) and AOD( $0.55 \mu\text{m}$ ) = 0.88 (C6)] and oasis [AOD( $0.55 \mu\text{m}$ ) = 0.85 (C5) and AOD( $0.55 \mu\text{m}$ ) = 0.86 (C6)] very well. When using adapted spectral slopes  $a_{0.65/2.1}$  and  $a_{0.47/0.65}$  in the C5 algorithm a good performance of the aerosol retrieval was also obtained for the urban surface type with AOD( $0.55 \mu\text{m}$ ) = 0.86, whereby the modified C6 algorithm tends to overestimate the AOD with AOD( $0.55 \mu\text{m}$ ) = 0.90. The largest discrepancies were found for the surface type Farmland where the brightness criterium in the MODIS retrieval is exceeded. For all methods (operational and modified) the retrieved AOD was significantly underestimated within a range of 0.61–0.71 compared to the reference value of 0.85.

## Adaption of the MODIS aerosol retrieval algorithm

E. Jäkel et al.

Title Page

Abstract

Introduction

Conclusions

References

Tables

Figures



Back

Close

Full Screen / Esc

Printer-friendly Version

Interactive Discussion



## Adaption of the MODIS aerosol retrieval algorithm

E. Jäkel et al.

Title Page

Abstract

Introduction

Conclusions

References

Tables

Figures

◀

▶

◀

▶

Back

Close

Full Screen / Esc

Printer-friendly Version

Interactive Discussion



The operational MODIS aerosol algorithms of Collections 5 and 6 retrieve the AOD within the expected uncertainty for densely vegetated surfaces, but shortcomings can be observed for higher reflecting urban areas and Farmland. The increased retrieval uncertainty for urban areas can be overcome by using spectral slopes suitable for urban surface within the algorithm. Changing the spectral slope parameter for urban surfaces improved the agreement between AOD(MODIS) and AOD(AERONET). The used spectral slopes in the modified algorithms were derived from airborne nadir radiance measurements, therefore we restricted the application of the retrieval methods to viewing sensor zenith angles of lower than 10°. For future studies we suggest to use airborne imaging spectrometer measurements to characterize the slope parameters for urban areas also for different viewing geometries than the nadir observation as applied in this study. This would allow corrections of the operational retrievals due to effect of the bidirectional reflectance distribution function (BRDF) also for other angles. Furthermore, an additional adaption of the  $a_{0.65/2.1}$  slope parameter would certainly enhance the retrieval quality.

*Acknowledgements.* This work was conducted within the scope of the German Research Foundation (DFG) priority program SPP 1233 „Megacities Megachallenge – Informal Dynamics of Global Change“(WE 1900/16-2). We thank our cooperation partners of the Institute of Remote Sensing and Digital Earth for providing the possibility to join their airborne field experiment in Zhongshan. Furthermore, we thank the Hong-Bin Chen and Philippe Goloub for their effort in establishing and maintaining the Beijing AERONET site.

## References

- Alpert, P., Shvainshtein, O., and Kishcha, P.: AOD trends over megacities based on space monitoring using MODIS and MISR, *American J. Climate Change*, 1, 117–131, doi:10.4236/ajcc.2012.13010, 2012. 7337
- Andrews, E., Sheridan, P. J., Fiebig, M., McComiskey, A., Ogren, J. A., Arnott, P., Covert, D., Elleman, R., Gasparini, R., Collins, D., Jonsson, H., Schmid, B., and Wang, J.: Compari-



## Adaption of the MODIS aerosol retrieval algorithm

E. Jäkel et al.

Title Page

Abstract

Introduction

Conclusions

References

Tables

Figures



Back

Close

Full Screen / Esc

Printer-friendly Version

Interactive Discussion



Mexico City urban area, *Atmos. Chem. Phys.*, 7, 5467–5477, doi:10.5194/acp-7-5467-2007, 2007. 7337, 7338

Drury, E., Jacob, D. J., Wang, J., Spurr, R., and Chance, K.: Improved algorithm for MODIS satellite retrievals of aerosol optical depths over western North America, *J. Geophys. Res.*, 113, D16204, doi:10.1029/2007JD009573, 2008. 7338

Dubovik, O. and King, M.: A flexible inversion algorithm for retrieval of aerosol optical properties from Sun and sky radiance measurements, *J. Geophys. Res.*, 105, 20673–20696, doi:10.1029/2000JD900282, 2000. 7343

Escribano, J., Gallardo, L., Rondanelli, R., and Choi, Y.-S.: Satellite retrievals of aerosol optical depth over a subtropical urban area: the role of stratification and surface reflectance, *Aerosol Air Qual. Res.*, 14, 596–U568, doi:10.4209/aaqr.2013.03.0082, 2014. 7338

Folberth, G. A., Rumbold, S. T., Collins, W. J., and Butler, T. M.: Global radiative forcing and megacities, *Urban Climate*, 1, 4–19, doi:10.1016/j.uclim.2012.08.001, 2012. 7337

Houghton, J., Ding, Y., Griggs, D., Noguer, M., van der Linden, P., Dai, X., Maskell, K., and Johnson, C.: *Climate CHANGE 2001: The Scientific Basis*, Tech. rep., Intergovernmental Panel on Climate Change (IPCC), IPCC Secretariat, c/o World Meteorological Organization, Geneva, Switzerland, 2001. 7337

Jacobson, M.: Strong radiative heating due to the mixing state of black carbon in atmospheric aerosols, *Nature*, 409, 695–697, doi:10.1038/35055518, 2001. 7337

Jäkel, E., Wendisch, M., and Mayer, B.: Influence of spatial heterogeneity of local surface albedo on the area-averaged surface albedo retrieved from airborne irradiance measurements, *Atmos. Meas. Tech.*, 6, 527–537, doi:10.5194/amt-6-527-2013, 2013. 7347

Kaufman, Y., Tanre, D., Remer, L., Vermote, E., Chu, A., and Holben, B.: Operational remote sensing of tropospheric aerosol over land from EOS moderate resolution imaging spectroradiometer, *J. Geophys. Res.*, 102, 17051–17067, doi:10.1029/96JD03988, 1997. 7337, 7340

Lawrence, M. G., Butler, T. M., Steinkamp, J., Gurjar, B. R., and Lelieveld, J.: Regional pollution potentials of megacities and other major population centers, *Atmos. Chem. Phys.*, 7, 3969–3987, doi:10.5194/acp-7-3969-2007, 2007. 7337

Levy, R., Remer, L., Mattoo, S., Vermote, E., and Kaufman, Y.: Second-generation operational algorithm: retrieval of aerosol properties over land from inversion of Moderate Resolution Imaging Spectroradiometer spectral reflectance, *J. Geophys. Res.*, 112, D13211, doi:10.1029/2006JD007811, 2007. 7337, 7340, 7348

## Adaption of the MODIS aerosol retrieval algorithm

E. Jäkel et al.

Title Page

Abstract

Introduction

Conclusions

References

Tables

Figures



Back

Close

Full Screen / Esc

Printer-friendly Version

Interactive Discussion



- Levy, R. C., Remer, L. A., Kleidman, R. G., Mattoo, S., Ichoku, C., Kahn, R., and Eck, T. F.: Global evaluation of the Collection 5 MODIS dark-target aerosol products over land, *Atmos. Chem. Phys.*, 10, 10399–10420, doi:10.5194/acp-10-10399-2010, 2010. 7337, 7351, 7353
- Levy, R. C., Mattoo, S., Munchak, L. A., Remer, L. A., Sayer, A. M., Patadia, F., and Hsu, N. C.: The Collection 6 MODIS aerosol products over land and ocean, *Atmos. Meas. Tech.*, 6, 2989–3034, doi:10.5194/amt-6-2989-2013, 2013. 7337, 7339, 7341
- Li, S. S., Chen, L. F., Tao, J. H., Hand, D., Wang, Z. T., Su, L., Fan, M., and Yu, C.: Retrieval of aerosol optical depth over bright targets in the urban areas of North China during winter, *Science China*, 55, 1545–1553, doi:10.1007/s11430-012-4432-1, 2012. 7338
- Mayer, B. and Kylling, A.: Technical note: The libRadtran software package for radiative transfer calculations - description and examples of use, *Atmos. Chem. Phys.*, 5, 1855–1877, doi:10.5194/acp-5-1855-2005, 2005. 7344
- Menon, S., Hansen, J., Nazarenko, L., and Luo, Y.: Climate effects of black carbon in China and India, *Science*, 297, 2250–2253, doi:10.1126/science.1075159, 2002. 7337
- Mielonen, T., Levy, R. C., Aaltonen, V., Komppula, M., de Leeuw, G., Huttunen, J., Lihavainen, H., Kolmonen, P., Lehtinen, K. E. J., and Arola, A.: Evaluating the assumptions of surface reflectance and aerosol type selection within the MODIS aerosol retrieval over land: the problem of dust type selection, *Atmos. Meas. Tech.*, 4, 201–214, doi:10.5194/amt-4-201-2011, 2011. 7337, 7351
- Oo, M., Jerg, M., Hernundes, E., Picón, A., Gross, B., Moshary, F., and Ahmed, S.: Improved MODIS aerosol retrieval using modified VIS/SWIR surface albedo ratio over urban scenes, *IEEE T. Geosci. Remote*, 48, 983–1000, doi:10.1109/TGRS.2009.2028333, 2010. 7337, 7338
- Ramanathan, V., Crutzen, P., Kiehl, J., and Rosenfeld, D.: Aerosols, climate, and the hydrological cycle, *Science*, 294, 2119–2124, doi:10.1126/science.1064034, 2001. 7337
- Schaaf, C. B., Gao, F., Strahler, A. H., Lucht, W., Li, X. W., Tsang, T., Strugnell, N. C., Zhang, X. Y., Jin, Y. F., Muller, J. P., Lewis, P., Barnsley, M., Hobson, P., Disney, M., Roberts, G., Dunderdale, M., Doll, C., d'Entremont, R. P., Hu, B. X., Liang, S. L., Privette, J. L., and Roy, D.: First operational BRDF, albedo nadir reflectance products from MODIS, *Remote Sens. Environ.*, 83, 135–148, doi:10.1016/S0034-4257(02)00091-3, 2002. 7337

## Adaption of the MODIS aerosol retrieval algorithm

E. Jäkel et al.

Title Page

Abstract

Introduction

Conclusions

References

Tables

Figures

◀

▶

◀

▶

Back

Close

Full Screen / Esc

Printer-friendly Version

Interactive Discussion



- Tegen, I., Koch, D., Lacis, A., and Sato, M.: Trends in tropospheric aerosol loads and corresponding impact on direct radiative forcing between 1950 and 1990: a model study, *J. Geophys. Res.*, 105, 26971–26989, doi:10.1029/2000JD900280, 2000. 7337
- Wendisch, M., Müller, D., Schell, D., and Heintzenberg, J.: An airborne spectral albedometer with active horizontal stabilization, *J. Atmos. Ocean. Tech.*, 18, 1856–1866, doi:10.1175/1520-0426(2001)018<1856:AASAWA>2.0.CO;2, 2001. 7342
- Wendisch, M., Pilewskie, P., Jäkel, E., Schmidt, S., Pommier, J., Howard, S., Jonsson, H. H., Guan, H., Schröder, M., and Mayer, B.: Airborne measurements of areal spectral surface albedo over different sea and land surfaces, *J. Geophys. Res.*, 109, D08203, doi:10.1029/2003JD004392, 2004. 7342, 7344
- Wong, M., Nichol, J., and Lee, K.: An operational MODIS aerosol retrieval algorithm at high spatial resolution, and its application over a complex urban region, *Atmos. Res.*, 99, 579–589, doi:10.1016/j.atmosres.2010.12.015, 2011. 7338
- Yu, X., Cheng, T., Chen, J., and Liu, Y.: Climatology of aerosol radiative properties in northern China, *Atmos. Res.*, 844, 132–141, doi:10.1016/j.atmosres.2006.06.003, 2007. 7337
- Zha, Y., Wang, Q., Yuan, J., Gao, J., Jiang, J., Lu, H., and Huang, J.: Improved retrieval of aerosol optical thickness from MODIS measurements through derived surface reflectance over Nanjing, China, *Tellus B*, 63, 952–958, doi:10.1111/j.1600-0889.2011.00545.x, 2011. 7338



Adaption of the  
MODIS aerosol  
retrieval algorithm

E. Jäkel et al.

**Table 2.** Relative uncertainties of the different error sources and uncertainty of surface albedo and reflectance after Gaussian error propagation for high aerosol particle optical depth. The roman numerals I–IV indicate the wavelength ranges. I: 0.4–0.6  $\mu\text{m}$ , II: 0.6–1.0  $\mu\text{m}$ , III: 1.0–1.8  $\mu\text{m}$ , IV: 1.8–2.1  $\mu\text{m}$ .

|                      | Sensitivity (%)  |     |      |      |  |      |     |     |      |
|----------------------|--|-----|------|------|--|------|-----|-----|------|
|                      | $\alpha_s(\lambda)$ , high optical depth<br>[AOD(0.53 $\mu\text{m}$ ) = 0.9] |     |      |      | $\rho_s(\lambda)$ , high optical depth<br>[AOD(0.53 $\mu\text{m}$ ) = 0.9] |      |     |     |      |
|                      | I  | II  | III  | IV   | I  | II   | III | IV  |      |
| $F_\lambda^\uparrow$ | 3.1  | 3.1 | 3.5  | 10.8 | $I^\uparrow$   | 6.6  | 6.6 | 9.5 | 14.4 |
| AOD                  | 25   | 19  | 9    | 0.8  | AOD  | 10   | 5   | 0.2 | 1.5  |
| $\tilde{\omega}$     | 20   | 7   | 4.5  | 0.9  | $\tilde{\omega}$   | 11   | 4   | 2.5 | 0.5  |
| $g$                  | 15   | 8   | 4.5  | 1.5  | $g$  | 8.5  | 3   | 2   | 0.3  |
| $z_F$                | 1  | 0.1 | 0.1  | 0.1  | $z_F$  | 1    | 0.1 | 0.1 | 0.1  |
| $\alpha_{s,\lambda}$ | 35.5   | 22  | 11.6 | 11   | $\rho_{s,\lambda}$   | 18.4 | 9.7 | 10  | 14.5 |

Title Page

Abstract Introduction

Conclusions References

Tables Figures

◀ ▶

◀ ▶

Back Close

Full Screen / Esc

Printer-friendly Version

Interactive Discussion



## Adaption of the MODIS aerosol retrieval algorithm

E. Jäkel et al.

**Table 3.** Overview of the slopes and intercepts for the calculation of the surface reflectance  $\rho_{s,0.46}$  and  $\rho_{s,0.47}$  following Eqs. (1) and (2) for different surface types used in the operational and modified algorithms C5 and C6. The C6 parameters are given in brackets when they differ from the C5 approach.

| Surface Type       | Operational Algorithm C5 (C6) |                 |                |                | Adapted Algorithm |                |
|--------------------|-------------------------------|-----------------|----------------|----------------|-------------------|----------------|
|                    | $a_{0.47/0.65}$               | $b_{0.47/0.65}$ | $a_{0.65/2.1}$ | $b_{0.65/2.1}$ | $a_{0.47/0.65}$   | $a_{0.65/2.1}$ |
| Kentucky Bluegrass | 0.49                          | 0.005           | 0.58 (0.48)    | -0.00143       | 1                 | 0.3            |
| Farmland           | 0.49                          | 0.005           | 0.48 (0.58)    | -0.00143       | 0.43              | 0.68           |
| Oasis              | 0.49                          | 0.005           | 0.51 (0.56)    | -0.00143       | 0.49              | 0.81           |
| Urban              | 0.49                          | 0.005           | 0.49 (0.59)    | -0.00143       | 0.8               | 0.8            |

Title Page

Abstract

Introduction

Conclusions

References

Tables

Figures

◀

▶

◀

▶

Back

Close

Full Screen / Esc

Printer-friendly Version

Interactive Discussion





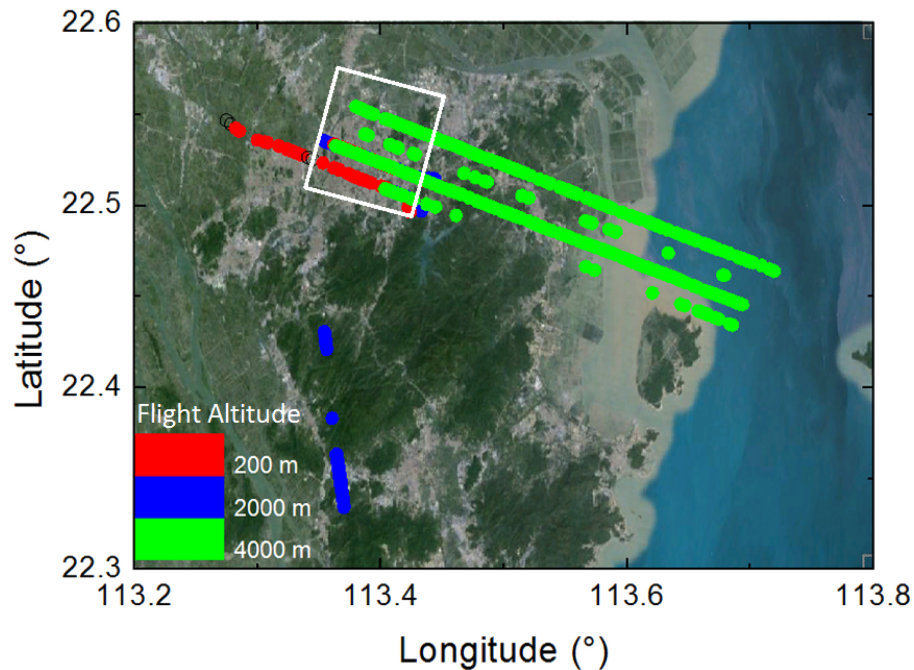


**Figure 1.** Flight pattern for the airborne measurements in Zhongshan on 03 December 2009. The area marked with the rectangle shows the position of the measurements which are averaged for the spatially-averaged surface albedo and surface reflectance spectra.

**Adaption of the MODIS aerosol retrieval algorithm**

E. Jäkel et al.

|                          |              |
|--------------------------|--------------|
| Title Page               |              |
| Abstract                 | Introduction |
| Conclusions              | References   |
| Tables                   | Figures      |
| ◀                        | ▶            |
| ◀                        | ▶            |
| Back                     | Close        |
| Full Screen / Esc        |              |
| Printer-friendly Version |              |
| Interactive Discussion   |              |





Adaption of the  
MODIS aerosol  
retrieval algorithm

E. Jäkel et al.

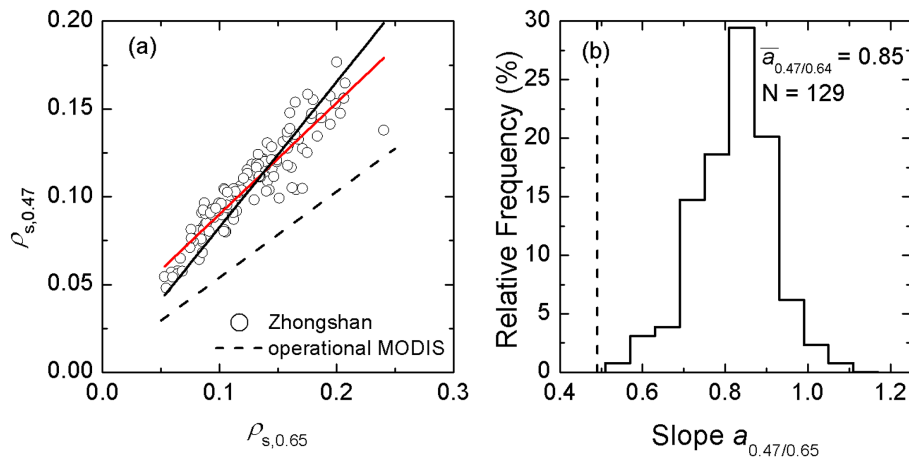


**Figure 3.** (a) Surface reflectance at 0.47 μm  $\rho_s(0.47 \mu\text{m})$  as function of surface reflectance at 0.65 μm  $\rho_s(0.65 \mu\text{m})$  for Zhongshan. The solid lines represent the linear fits of the measured data with (red) and without (black) an intercept. The dependency of  $\rho_s(0.47 \mu\text{m})$  and  $\rho_s(0.65 \mu\text{m})$  in the operational algorithm is shown as dashed line. (b) Relative frequency distribution for all possible ratios of  $\rho_s(0.47 \mu\text{m})$  and  $\rho_s(0.65 \mu\text{m})$  representing the slope  $a_{0.47/0.65}$  for zero y-intercept. The slope of the operational algorithm is shown as dashed line.

Adaption of the  
MODIS aerosol  
retrieval algorithm

E. Jäkel et al.

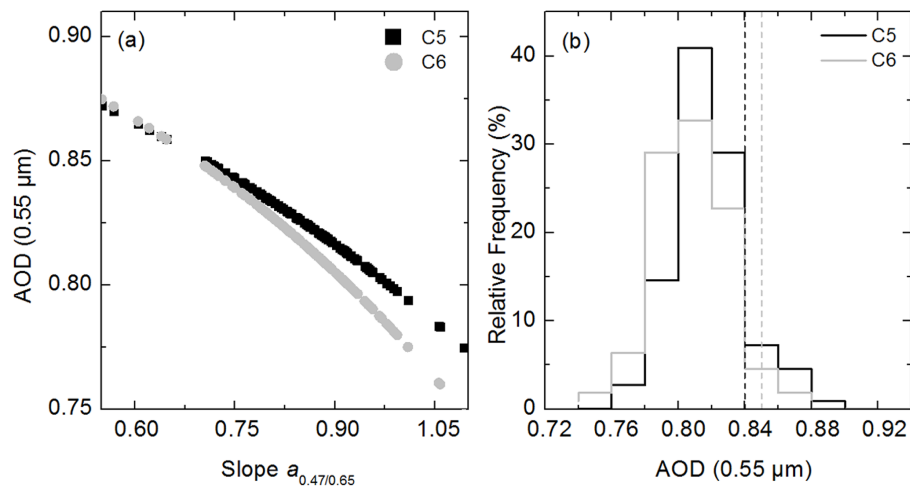


**Figure 4.** (a) Correlation between slope  $a_{0.47/0.65}$  used for the AOD retrieval and the resulting AOD at 0.55  $\mu\text{m}$  for Zhongshan for the C5 and the C6 algorithm applied for measurements on 01 December 2009. (b) Relative frequency distribution of retrieved AOD for Zhongshan for the modified C5 and C6 code. The corresponding AOD of the unchanged operational retrievals is shown as vertical lines.

[Title Page](#)[Abstract](#)[Introduction](#)[Conclusions](#)[References](#)[Tables](#)[Figures](#)[◀](#)[▶](#)[◀](#)[▶](#)[Back](#)[Close](#)[Full Screen / Esc](#)[Printer-friendly Version](#)[Interactive Discussion](#)

Adaption of the  
MODIS aerosol  
retrieval algorithm

E. Jäkel et al.

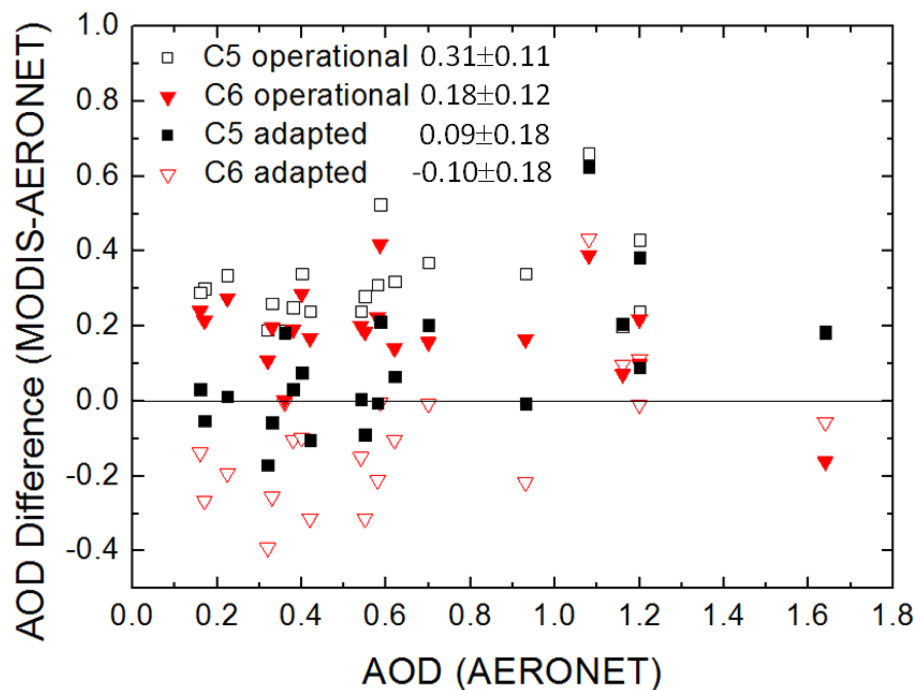


**Figure 5.** Deviation of AOD retrieved from MODIS data using the operational and adapted collection 5 and 6 method and the AERONET data for Beijing. The mean difference and standard deviation of the differences are also listed in the figure.

Title Page

Abstract

Introduction

Conclusions

References

Tables

Figures



Back

Close

Full Screen / Esc

Printer-friendly Version

Interactive Discussion





Adaption of the  
MODIS aerosol  
retrieval algorithm

E. Jäkel et al.

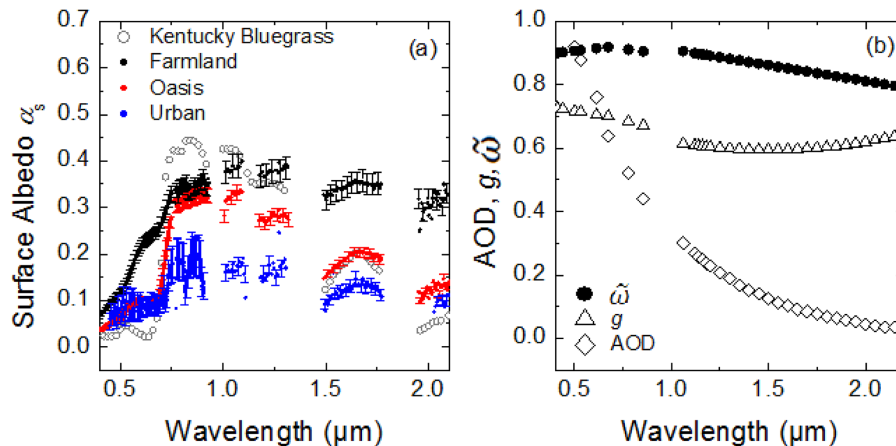


**Figure 7.** (a) Surface albedo spectra of different surface types. For urban, Oasis and farmland the measurement uncertainty is given as vertical error bars. (b) Spectral characteristic of the optical aerosol properties used in the model study.